SESAM Mode-Locked Yb:Ca3Gd2(BO3)4 Femtosecond Laser

Huang-Jun Zeng, Zhang-Lang Lin, Wen-Ze Xue, Ge Zhang, Zhongben Pan, Haifeng Lin, Pavel Loiko, Xavier Mateos, Valentin Petrov, Li Wang, et al.

applied sciences

MDPI

Article

SESAM mode-locked Yb:$Ca_3Gd_2(BO_3)_4$ femtosecond laser

Huang-Jun Zeng [1,2], Zhang-Lang Lin [2], Wen-Ze Xue [2], Ge Zhang [2], Zhongben Pan [3], Haifeng Lin [4], Pavel Loiko [5], Xavier Mateos [6,#], Valentin Petrov [7], Li Wang [7] and Weidong Chen [2,7,*]

[1] College of Chemistry, Fuzhou University, Fuzhou, 350002 Fujian, China; zenghuangjun@fjirsm.ac.cn (H.J.Z.)
[2] Fujian Institute of Research on the Structure of Matter, Chinese Academy of Sciences, Fuzhou, 350002 Fujian, China; linzl@fjirsm.ac.cn (Z.L.L.); xuewenze@fjirsm.ac.cn (W.Z.X.); zhg@fjirsm.ac.cn (G.Z.); chenweidong@fjirsm.ac.cn (W.C.)
[3] Institute of Chemical Materials, China Academy of Engineering Physics, Mianyang, 621900 Sichuan, China; pzb8625@126.com (Z.P.)
[4] College of Physics and Optoelectronic Engineering, Shenzhen University, Shenzhen, 518118 Guangdong, China; h.f.lin@szu.edu.cn (H.L.)
[5] Centre de Recherche sur les Ions, les Matériaux et la Photonique (CIMAP), UMR 6252 CEA-CNRS-ENSICAEN, Université de Caen Normandie, 6 Boulevard Maréchal Juin, 14050 Caen Cedex 4, France; pavel.loiko@ensicaen.fr (P.L.)
[6] Universitat Rovira i Virgili (URV), Física i Cristal·lografia de Materials i Nanomaterials (FiCMA-FiCNA), Marcel.li Domingo 1, 43007 Tarragona, Spain; [#]Serra Húnter Fellow; xavier.mateos@urv.cat (X.M.)
[7] Max Born Institute for Nonlinear Optics and Short Pulse Spectroscopy, Max-Born-Str. 2a, 12489 Berlin, Germany; petrov@mbi-berlin.de (V.P.); Li.Wang@mbi-berlin.de (L.W.); chenweidong@fjirsm.ac.cn (W.C.)
* Correspondence: chenweidong@fjirsm.ac.cn

Abstract: We report on the first passively mode-locked femtosecond laser operation of a disordered Yb:$Ca_3Gd_2(BO_3)_4$ crystal using a SEmiconductor Saturable Absorber Mirror (SESAM). Pumping with a single-transverse mode fiber-coupled laser diode at 976 nm, nearly Fourier-transform limited pulses as short as 96 fs are generated at 1045 nm with an average output power of 205 mW and a pulse repetition rate of ~67.3 MHz. In the continuous-wave regime, high slope efficiency up to 59.2% and low laser thresholds down to 25 mW are obtained. Continuous wavelength tuning between 1006 – 1074 nm (a tuning range of 68 nm) is demonstrated. Yb:$Ca_3Gd_2(BO_3)_4$ crystals are promising for the development of ultrafast lasers at ~1 μm.

Keywords: Ultrafast laser; Solid-state laser; Ytterbium laser; Mode-locking.

Citation: Lastname, F.; Lastname, F.; Lastname, F. Title. *Appl. Sci.* **2021**, *11*, x. https://doi.org/10.3390/xxxxx

Academic Editor: Firstname Lastname

Received: date
Accepted: date
Published: date

1. Introduction

Ytterbium (Yb^{3+}) doped crystals are attractive for the development of power-scalable, wavelength-tunable and ultrafast coherent light sources emitting at the wavelength of ~1 μm. Yb^{3+} ions feature a simple electronic level scheme consisting of only two multiplets leading to higher laser slope efficiencies and weaker heat loading (as compared to Nd^{3+} ions) [1]. Yb^{3+}-doped crystals can be efficiently pumped by commericially available high-power InGaAs diode lasers emitting at 0.94 – 0.98 μm. For generation of ultrashort pulses in the sub-100 fs time domain, it is advantageous to use Yb^{3+}-doped crystals exhibiting structure disorder leading to strong inhomogeneous broadening of the Yb^{3+} absorption and emission bands [2-4]. In this way, smooth and broad gain profiles are accessible. It is still interesting to search for novel disordered crystals for Yb^{3+} doping combining large total Stark splitting of the ground-state $^2F_{7/2}$ (leading to broader emission range) and good thermal properties (allowing for power scalable laser operation).

Among the laser host crystals suitable for Yb^{3+} doping, double borates [e.g., $REAl_3(BO_3)_4$, $RECa_4O(BO_3)_3$, etc., where RE denotes a passive rare-earth ion] are attracting a lot of attention. They are characterized by a relatively large ground-state splitting [~1000 cm^{-1} for $GdCa_4O(BO_3)_3$] resulting from strong crystal fields, good thermo-optical [5] and

mechanical properties, high Yb^{3+} doping concentration (few tens at.%) that can be achieved and attractive nonlinear optical properties making them suitable, e.g., for self-frequency doubling. Monoclinic calcium RE oxoborates $Yb:YCa_4O(BO_3)_3$ are a good example of such crystals that exhibit local structure disorder leading to smooth and broad gain profiles extending up to 1.1 μm. Such advantages make them very suitable for high-power operation in the continuous-wave (CW) regime [6-8], as well as the design of broadband widely tunable and mode-locked (ML) lasers operation at ~1 μm [9, 10]. A diode-pumped $Yb:GdCa_4O(BO_3)_3$ (abbreviated: Yb:GdCOB) laser ML by a SESAM generated 90 fs pulses at ~1046 nm corresponding to an average output power of 40 mW at a pulse repetition rate of 100 MHz [10].

Recently, another calcium borate crystal family with a chemical formula $Ca_3RE_2(BO_3)_4$, where RE = Y, Lu, Gd and La, attracted attention for Yb^{3+} doping [11-14]. These crystals belong to the orthorhombic class with the space group *Pnma* and they are structurally disordered. Thus, Yb^{3+}-doped $Ca_3Gd_2(BO_3)_4$ crystal (abbreviated Yb:GdCB) with high optical quality has been successfully grown by the Czochralski method and laser performance in the CW regime has been characterized [11, 15, 16]. In the GdCB structure, the Ca^{2+} and Gd^{3+} cations statistically occupy three non-equivalent crystallographic sites forming M-oxygen distorted polyhedrons [17] (the dopant Yb^{3+} ions are expected to replace for the Gd^{3+} ones). This leads to a "glassy-like" spectroscopic behavior of Yb:GdCB crystals at the expense of a relatively low thermal conductivity of 0.92 W/mK at room temperature [18]. Pumping with a multi-transverse mode, fiber-coupled laser diode at 976 nm, a maximum CW output power of 1.4 W was obtained at ~1060 nm with a relatively low slope efficiency of 23.7% and high laser threshold of 900 mW [16]. Self-Q switched operation was also reported [19]. However, there is no report on a passively ML operation of Yb:GdCB laser to date.

In the present work, we report on the laser performance of the disordered Yb:GdCB crystal in the CW and the passively ML regimes. Pumping with a single-transverse mode, fiber-coupled laser diode, nearly Fourier-transform limited pulses as short as 96 fs were generated using a SESAM. To the best of our knowledge, this is the first report on the ML operation of the Yb:GdCB crystal.

2. Experimental setup

The experimental configuration of the Yb:GdCB laser is shown in Fig. 1. A high-quality crystal was grown by the Czochralski method with a measured Yb^{3+} concentration of 5 at.%.

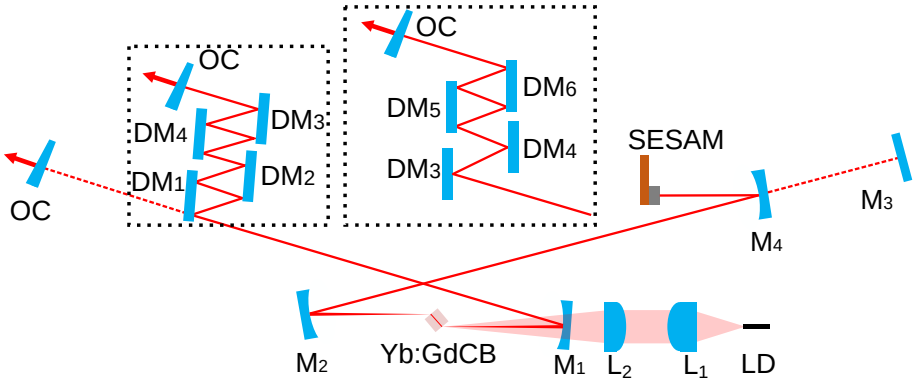

Figure 1. Schematic of the Yb:GdCB laser. LD: fiber-coupled laser diode; L_1: aspherical lens; L_2: achromatic doublet lens; M_1, M_2 and M_4: concave mirrors; M_3: flat rear mirror for CW operation; DM_1 – DM_6: dispersive mirrors; OC: output coupler; SESAM: SEmiconductor Saturable Absorber Mirror.

Yb:GdCB belongs to the orthorhombic class and its lattice constants are a =7.1937 Å, b = 15.5311 Å and c = 8.6140 Å. Here, we use the notations of the standard *Pnma* crystallographic setting. The laser crystal was cut along the ***a***-axis with an aperture of 4 mm × 4 mm and a thickness of 3 mm. The input and output faces were polished to laser quality and left uncoated. The crystal was mounted on a copper holder without active cooling and placed between two dichroic folding mirrors M_1 and M_2 (radius of curvature, RoC = -100 mm) with the Brewster angle minimum loss condition fulfilled for both the laser and the pump beams. CW and ML laser operation of the Yb:GdCB crystal were evaluated with an X-folded astigmatically compensated linear cavity. The crystal orientation determined the laser polarization $\boldsymbol{E} \parallel \boldsymbol{c}$ (due to its higher gain compared to $\boldsymbol{E} \parallel \boldsymbol{b}$). The pump source was a non-polarized fiber-coupled laser diode emitting a nearly diffraction-limited beam with a propagation factor (M^2) of ~1.02. The laser diode had a Fiber Bragg Grating (FBG) for wavelength locking at 976 nm over the entire operation range with an emission bandwidth (full width at half-maximum, FWHM) of 0.2 nm, which well matched the bandwidth of the zero-phonon-line in the absorption spectrum of the Yb:GdCB crystal. Given the transmissions of the pump reimaging lenses and the pump mirror M_1, the maximum incident pump power on the laser crystal was 1.29 W. The use of the single-transverse mode laser diode with nearly diffraction-limited beam led to higher gain per watt of absorbed pump power due to improved mode-matching and the lowest thermal stress in the laser crystal (as compared to pumping by fiber-coupled diodes with a "top-hat" beam profile). This allowed us to optimize the Yb laser for low threshold and high efficiency operation in the CW regime, and also for femtosecond pulse generation in the ML regime. The pump beam was collimated by an aspherical lens L_1 (f = 26 mm) and focused into the laser crystal through the M_1 mirror using an achromatic doublet lens L_2 (f = 100 mm) resulting in a beam waist radius of 18.7 and 36.9 μm in the sagittal and tangential planes, respectively.

3. Continuous-wave laser operation

In the CW regime, the laser performance of the Yb:GdCB crystal was evaluated with a four-mirror cavity including a flat rear mirror M_3 and an output coupler (OC) without SESAM, as shown in Fig. 1.

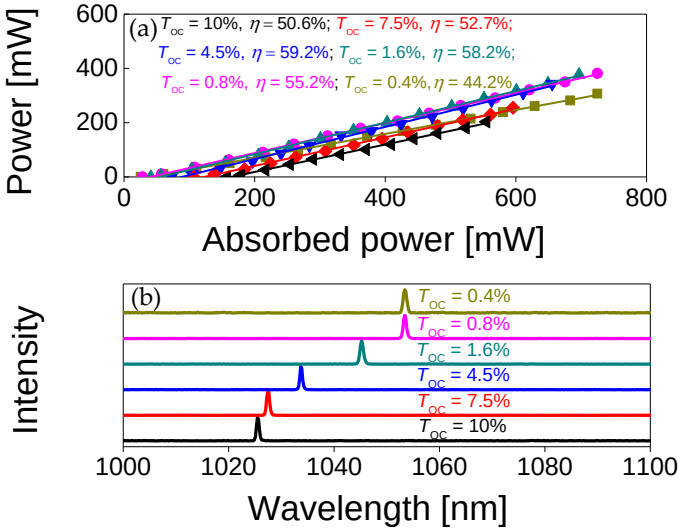

Figure 2. CW laser performance of ***a***-cut Yb:GdCB crsytal: (a) input-output dependences for different transmission of the OC (T_{OC}), η – slope efficiency; (b) laser spectra. The laser polarization is $\boldsymbol{E} \parallel \boldsymbol{c}$.

The cavity mode size in the laser crystal was estimated by the ABCD formalism yielding a waist radius of 21 and 37 μm in the sagittal and tangential planes, respectively. As shown in Fig. 2(a), a maximum output power of 382 mW was achieved for OC with a

transmission at the laser wavelength T_{OC} = 0.8% at an absorbed pump power of 725 mW, corresponding to a laser threshold of only 25 mW and a slope efficiency of 55.2%. The maximum slope efficiency of 59.2% was obtained for higher T_{OC} = 4.5%. The laser threshold gradually increased with T_{OC} (0.4% - 7.5%), from 25 to 158 mW. The measured single-pass pump absorption under lasing conditions tended to decrease with T_{OC} between 56.2% to 43%, indicating a certain ground-state bleaching and its suppression by the recycling effect. The emission wavelength of the Yb:GdCB laser in the CW regime experienced a blue-shift with increasing transmission of the OC, from 1025.5 to 1053.4 nm, see Fig. 2(b). This behavior is due to the quasi-three-level nature of the Yb laser scheme.

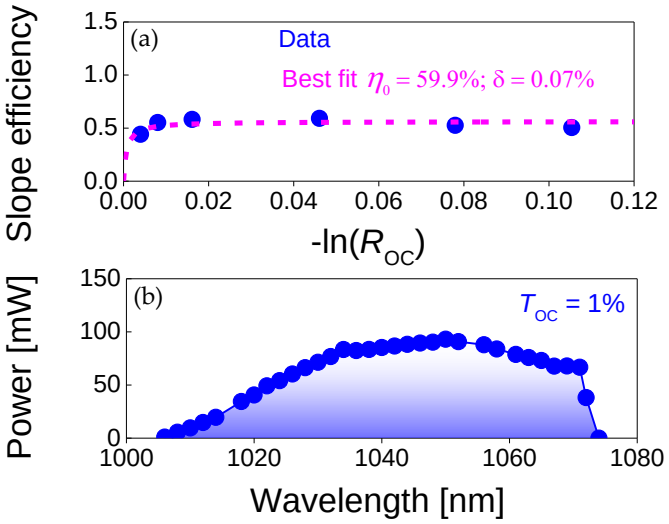

Figure 3. (a) Caird analysis for the CW Yb:GdCB laser: slope efficiency as a function of the OC reflectivity R_{OC} = 1 - T_{OC}; (b) wavelength tuning curve obtained with a SF-10 Brewster prism placed between M_1 and the OC with T_{OC} = 1%.

The Caird analysis [20] was applied to estimate the total losses δ (including cavity and laser crystal but excluding reabsorption effects) and the intrinsic slope efficiency η_0 through fitting the measured laser slope efficiency as a function of the reflectivity of the OC, R_{OC} = 1 – T_{OC} with the following equation:

$$\eta = \eta_0 \frac{\lambda_p}{\lambda_l} \frac{-\ln(R_{OC})}{\delta - \ln(R_{OC})} \quad (1)$$

where λ_p and λ_l are the pump and laser wavelengths, respectively. The best fit gave round trip cavity losses of δ = 0.07% and an intrinsic slope efficiency of η_0 = 59.9%, see Fig. 3(a). The extremely low cavity losses are evidence for good quality of the laser crystal and well-optimized cavity alignment.

A SF-10 Brewster prism was inserted close to the OC for wavelength tuning in the CW regime. With a 1% OC, a broad range of continuous wavelength tuning, about 68 nm, was obtained, as shown in Fig. 3(b).

4. SESAM mode-locked operation

For passively ML operation, the rear mirror M_3 was replaced by a plane-concave mirror M_4 with RoC = -100 mm to create a second beam waist on the SESAM ensuring its efficient bleaching. The estimated radius of this second beam waist was 60 and 65 μm in the sagittal and tangential planes, respectively. The SESAM (BATOP, GmbH) applied in this experiment had a relaxation time constant of ~1 ps and a modulation depth of 1.2%. The intracavity group delay dispersion (GDD) was managed by implementing four flat dispersive mirrors (DMs, characterized by the following GDD per bounce: DM_1 = -100 fs^2,

DM_2 = -100 fs², DM_3 = DM_4= -250 fs², DM_5 = DM_6= -55 fs²) in the other cavity arm. The total negative GDD value was varied by changing the number of bounces on the DMs.

Initially, the ML operation was investigated by applying eight bounces (single pass) on the DMs (DM_1 – DM_4), as shown in Fig. 1, yielding a total round-trip negative GDD of -2800 fs². Stable and self-starting ML operation was achieved with the 1.6% OC. The sech²-shaped spectrum of the soliton pulses was centered at 1052 nm with a FWHM of 8.2 nm, as shown in Fig. 4(a). The measured SHG-based intensity autocorrelation trace gave a pulse duration of 146 fs by assuming a sech²-shape temporal profile, see Fig. 4(b). This results in a time-bandwidth product (TBP) of 0.324 which is slightly above the Fourier transform-limited value for a sech²-shaped temporal profile. The long-scale SHG-based intensity autocorrelation scan of 50 ps indicates a single-pulse operation without any pedestals or multi-pulses, see inset in Fig 4(b). The maximum average output power amounted to 181 mW at an absorbed pump power of 697 mW. The corresponding peak power was ~17.5 kW at a pulse repetition rate of 62.4 MHz. The optical conversion efficiency reached 26% with respect to the absorbed pump power.

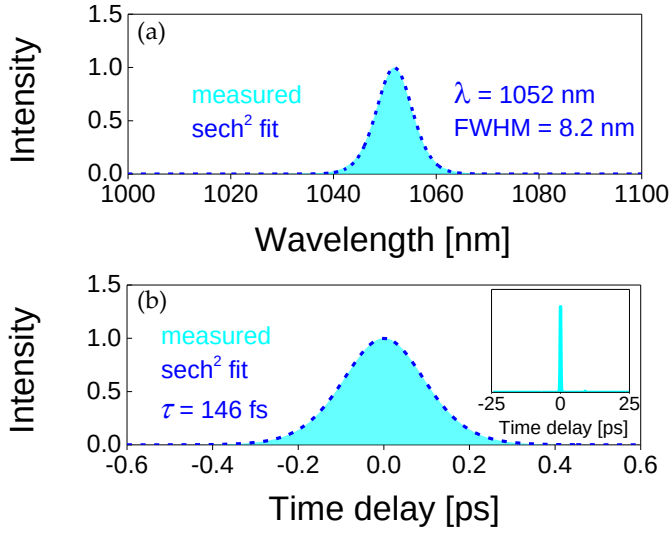

Figure 4. SESAM ML Yb:GdCB laser with T_{OC} = 1.6%. (a) Optical spectrum and (b) SHG-based intensity autocorrelation trace with a sech² fit. *Inset*: simultaneously measured long-scale SHG-based intensity autocorrelation trace for the time span of 50 ps.

The pulse duration was further shortened by optimizing the total negative GDD value. The shortest pulse duration was achieved by applying six bounces (single pass) on the DMs (DM_3 – DM_6), as shown in Fig. 1, yielding a total negative GDD of -1620 fs². Self-starting ML operation of the Yb:GdCB laser with a 2.5% OC produced soliton pulses at the central wavelength of 1045 nm with a spectral FWHM of 12.1 nm, as depicted in Fig. 5(a). Pulses as short as 96 fs were achieved as shown by the measured SHG-based intensity autocorrelation trace in Fig. 5(b). The corresponding TBP of 0.319 indicates generation of nearly Fourier-transform limited pulses with a sech²-shaped temporal profile. A long-scale SHG-based intensity autocorrelation scan of 50 ps shown in the inset of Fig. 5(b), confirmed a single-pulse ML operation. The maximum average output power amounted to 205 mW at an absorbed pump power of 696 mW, which corresponded to an efficiency of 29.5%. The soliton pulses had a peak power of 28 kW at a pulse repetition rate of 67.3 MHz.

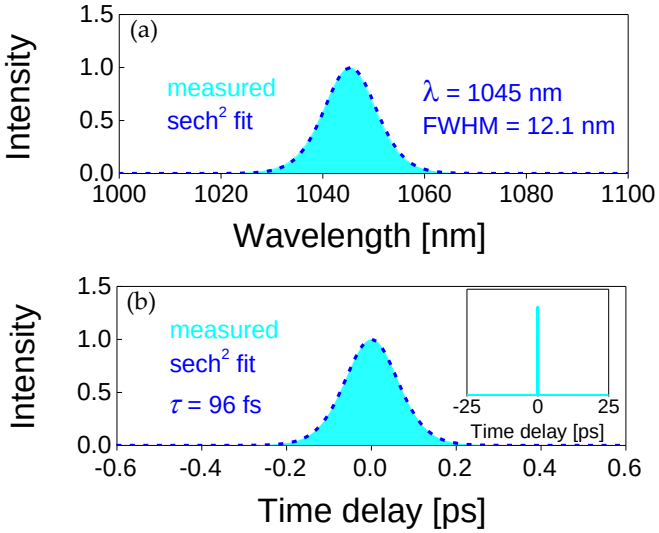

Figure 5. SESAM ML Yb:$Ca_3Gd_2(BO_3)_4$ laser with T_{OC} = 2.5%. (a) Optical spectrum and (b) SHG-based intensity autocorrelation trace with a sech² fit. *Inset*: simultaneously measured long-scale SHG-based intensity autocorrelation trace for the time span of 50 ps.

The steady-state pulse train corresponding to the shortest pulses achieved was characterized by a radio-frequency (RF) spectrum analyzer. The first beat note was recorded at ~67.3 MHz with a resolution bandwidth (RBW) of 300 Hz, as shown in Fig. 6(a). No spurious modulations could be observed with a signal-to-noise ratio above 76 dBc. This, together with the uniform 1-GHz harmonic beat notes shown in Fig. 6(b) is an evidence for stable CW mode-locking of the Yb:GdCB laser without any Q-switching or multiple pulsing instabilities.

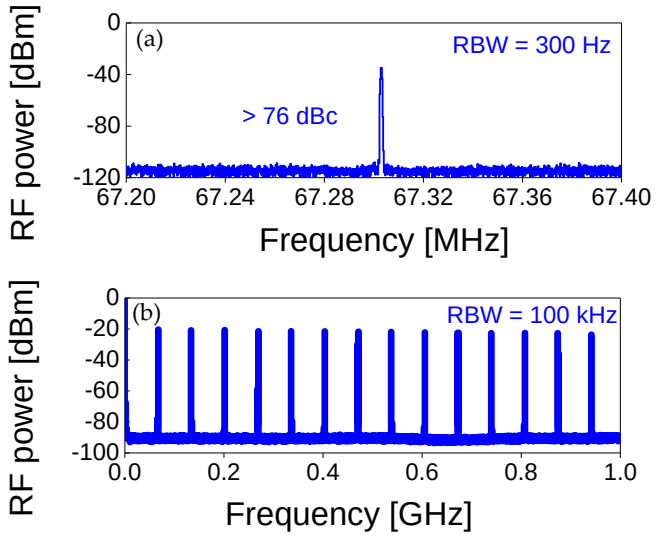

Figure 6. Radio-frequency (RF) spectra of the SESAM ML Yb:GdCB laser: (a) fundamental beat note at 67.3 MHz recorded a resolution bandwidth (RBW) of 300 Hz, and (b) harmonics on a 1-GHz frequency span, measured with a RBW of 100 kHz.

5. Conclusion

In conclusion, we present a comprehensive characterization of a diode-pumped Yb:GdCB laser operating both in the CW and passively ML regimes. Pumped with a single-transverse mode, fiber-coupled laser diode at 976 nm, the CW laser generated a maximum output power of 382 mW at 1053. nm corresponding to a very low threshold of 25 mW and high slope efficiency of 55.2%. Continuous wavelength tuning between

1006 and 1074 nm (a tuning range of 68 nm) was achieved. A SESAM ML Yb:GdCB laser emitted pulses as short as 96 fs at a central wavelength of 1045 nm with an average output power of 205 mW and a pulse repetition of ~67.3 MHz. To the best of our knowledge, this is the first report on passively ML operation of the Yb:GdCB crystal. Our results indicate the possibility for power scaling and pulse shortening accessing the sub-50 fs time domain for Yb:GdCB lasers by using high-power laser diodes and the Kerr-lens mode-locking technique.

Author Contributions: Conceptualization, W.C. and H.L.; methodology, G.Z. and L.W.; validation, Z.L.L., W.Z.X. and H.J.Z.; investigation, H.J.Z. and W.C.; resources, Z.P.; writing—original draft preparation, H.J.Z. and W.C.; writing—review and editing, P.L., X.M., L.W. and V.P.; supervision, W.C.; project administration, W.C.; funding acquisition, G.Z. All authors have read and agreed to the published version of the manuscript.

Funding: This research was funded by the National Natural Science Foundation of China (61975208, 51761135115, 61850410533, 62075090, 52032009, 52072351); Sino-German Scientist Cooperation and Exchanges Mobility Program (M-0040); Foundation of the President of China Academy of Engineering Physics (YZJJLX2018005); Foundation of Key Laboratory of Optoelectronic Materials Chemistry and Physics, Chinese Academy of Sciences (2008DP173016), Foundation of State Key Laboratory of Crystal Materials, Shandong University (KF2001).

Institutional Review Board Statement: Not applicable.

Informed Consent Statement: Not applicable.

Data Availability Statement: All of the data reported in the paper are presented in the main text. Any other data will be provided on request.

Conflicts of Interest: The authors declare no conflict of interest.

References

1. Chenais, S.; Druon, F.; Forget, S.; Balembois, F.; Georges, P. On thermal effects in solid-state lasers: The case of ytterbium-doped materials. Prog. Quantum. Electron. **2006**, 30, 89-153.

2. Cortes, A.G.; Torres, J M.C.; Han, X.; Cascales, C.; Zaldo, C.; Mateos, X.; River, S.; Griebner, U.; Petrov, V.; Valle, F.J. Tunable continuous wave and femtosecond mode-locked Yb^{3+} laser operation in $NaLu(WO_4)_2$. J. Appl. Phys. **2007**, 101, 063110.

3. Sévillano, P.; Georges, P.; Druon, F.; Descamps, D.; Cormier, E. 32-fs Kerr-lens mode-locked Yb:$CaGdAlO_4$ oscillator optically pumped by a bright fiber laser. Opt. Lett. **2014**, 39, 6001-6004.

4. Serrano, M.; Pérez, J.O.Á.; Zaldo, C.; Sanz, J.; Sobrados, I.; Alonso, J.; Cascales, C.; Díaz, M.F.; Jezowski, A.; Design of Yb^{3+} optical bandwidths by crystallographic modification of disordered calcium niobium gallium laser garnets. J. Mater. Chem. C. **2017**, 5, 11481-11495.

5. Loiko, P.; Mateos, X.; Wang, Y.; Pan, Z.; Yumashev, K.; Zhang, H.; Griebner, U.; Petrov, V. Thermo-optic dispersion formulas for YCOB and GdCOB laser host crystals. Opt. Mater. Express **2015**, 5, 1089-1097.

6. Chen, X.W.; Wang, L.S.; Liu, J.H.; Guo, Y.F.; Han, W.J.; Xu, H.H.; Yu, H.H.; Zhang, H.J. High-power CW and passively Q-switched laser operation of Yb:$GdCa_4O(BO_3)_3$ crystal. Opt. Laser Technol. **2016**, 79, 74-78.

7. Liu, J.H.; Han, W.J.; Chen, X.W.; Dai, Q.B.; Yu, H.H.; Zhang, H.J. Continuous-wave and passive Q-switching laser performance of Yb:$GdCa_4O(BO_3)_3$ crystal. IEEE J. Sel. Top. Quantum Electron. **2015**, 21, 1600808.

8. Loiko, P.; Serres, J.M.; Mateos, X.; Yu, H.; Zhang, H.J.; Liu, J.H.; Yumashev, K.; Griebner, U.; Petrov, V.; Aguilo, M.; Diaz, F. Thermal lensing and multiwatt microchip laser operation of Yb:YCOB Crystals. IEEE Photon. J. **2016**, 8, 1501312.

9. Yoshida, A.; Schmidt A.,; Petrov, V.; Fiebig, C.; Erbert, G.; Liu, J.H.; Zhang, H.J.; Wang, J.Y.; Griebner, U. Diode-pumped mode-locked Yb:YCOB laser generating 35 fs pulses. Opt. Lett. **2011**, 36, 4425-4427.

10. Druon, F.; Balembois, F.; Georges, P.; Brun, A.; Courjaud, A.; Honninger, C.; Salin, F.; Aron, A.; Mougel, F.; Aka, G.; Vivien, D. Generation of 90-fs pulses from a mode-locked diode-pumped Yb^{3+}:$Ca_4GdO(BO_3)_3$ laser. Opt. Lett. **2000**, 25, 423-425.

11. Haumesser, P.H.; Gaumé, R.; Benitez, J.M.; Viana, B.; Ferrand, B.; Aka, G.; Vivien, D.; Czochralski growth of six Yb-doped double borate and silicate laser materials. J. Cryst. Growth **2001**, 233, 233-242.

12. Wang, L.S.; Xu, H.H.; Pan, Z.B.; Han, W.J.; Chen, X.W.; Liu, J.H.; Yu, H.H.; Zhang, H.J. Anisotropic laser properties of Yb:$Ca_3La_2(BO_3)_4$ disordered crystal. Opt. Mater. **2016**, 58, 196-202.

13. Pan, Z.; Cai, H.; Huang, H.; Yu, H.; Zhang, H.; Wang, J. Growth, thermal properties and laser operation of a novel disordered Yb:$Ca_3La_2(BO_3)_4$ laser crystal. Opt. Mater. **2014**, 36, 2039-2043.

14. Brenier, A.; Tu, C.; Wang, Y.; You, Z.; Zhu, Z.; Li, J. Diode-pumped laser operation of Yb^{3+}-doped $Y_2Ca_3B_4O_{12}$ crystal. J. Appl. Phys. **2008**, 104, 013102.

15. Tu, C.; Wang, Y.; You, Z.; Li, J.; Zhu, Z.; Wu, B. Growth and spectroscopic characteristics of $Ca_3Gd_2(BO_3)_4$:Yb^{3+} laser crystal. J. Cryst. Growth **2004**, 265, 154-158.

16. Xu, J.L.; Tu, C.Y.; Wang, Y.; He, J.L. Multi-wavelength continuous-wave laser operation of Yb:$Ca_3Gd_2(BO_3)_4$ disordered crystal. Opt. Mater. **2011**, 33, 1766-1769 (2011).

17. Kosyl, K.M.; Paszkowicz, W.; Minikayev, R.; Shekhovtsov, A.N.; Kosmyna, M.B.; Chrunik, M.; Fitch, A.N. Site-occupancy scheme in disordered $Ca_3RE_2(BO_3)_4$: a dependence on rare-earth (RE) ionic radius. Acta Crystallogr. B. **2021**, 77, 339-346.

18. Gudzenko, L.; Kosmyna, M.; Shekhovtsov, A.; Paszkowicz, W.; Sulich, A.; Domagała, J.; Popov, P.; Skrobov, S.; Crystal Growth and Glass-Like Thermal conductivity of $Ca_3RE_2(BO_3)_4$ (RE= Y, Gd, Nd) single crystals. Crystals **2017**, 7, 88, 703008.

19. Xu, J.L.; Ji, Y.X.; Wang, Y.Q.; You, Z.Y.; Wang, H.Y.; Tu, C.Y. Self-Q-switched, orthogonally polarized, dual-wavelength laser using long-lifetime Yb^{3+} crystal as both gain medium and saturable absorber. Opt. Express, **2014**, 22, 6577-6585.

20. Caird, J.A.; Payne, S.A.; Staver, P.R.; Ramponi, A.; Chase, L. Quantum electronic properties of the $Na_3Ga_2Li_3F_{12}$:Cr^{3+} laser. IEEE J. Quantum Electron. **1988**, 24, 1077-1099.